ECS | The Electrochemical Society
Advancing solid state & electrochemical science & technology

A Facile, Dry-Processed Lithium Borate-Based Cathode Coating for Improved All-Solid-State Battery Performance

To cite this article: Erik A. Wu *et al* 2020 *J. Electrochem. Soc.* **167** 130516

View the article online for updates and enhancements.

A Facile, Dry-Processed Lithium Borate-Based Cathode Coating for Improved All-Solid-State Battery Performance

Erik A. Wu,[1,=] Chiho Jo,[1,2,=] Darren H. S. Tan,[1] Minghao Zhang,[1,*] Jean-Marie Doux,[1] Yu-Ting Chen,[3] Grayson Deysher,[3] and Ying Shirley Meng[1,2,4,**,z]

[1]*Department of Nano-Engineering, University of California San Diego, La Jolla, California 92093, United States of America*
[2]*LG Chem Research Park, Battery R&D, Daejeon, Republic of Korea*
[3]*Department of Materials Science and Engineering, University of California San Diego, La Jolla, California 92093, United States of America*
[4]*Sustainable Power & Energy Center (SPEC), University of California San Diego, La Jolla, California 92093, United States of America*

Sulfide-based solid electrolytes are known to have narrow electrochemical windows which limit their practical use in all-solid-state batteries (ASSBs). Specifically, when paired with a high-voltage transition metal oxide (TMO) cathode, the electrolyte will typically undergo unwanted degradation via chemical reactions or electrochemical oxidation, especially upon charging to voltages beyond the electrochemical stability window of the electrolyte. To mitigate these undesired reactions, thin (<10 nm), conformal, ionically-conducting, and electronically-insulating oxide-based protective coating layers have been applied on the cathode, typically via a solution process. In this work, a lithium borate-based (LBO) coating, prepared instead with a dry coating process, was shown to have the same beneficial properties. As evidenced by electrochemical characterization, the developed LBO coating shows good cycling performance and even performs better than the $LiNbO_3$ coating commonly used in the literature. This new solvent-free coating method can thus be used to fabricate longer-lasting ASSBs.

All-solid-state batteries (ASSBs) have gained much research interest due to their potential for higher energy density, the possibility of using metallic anodes, and improved safety since the solid-state electrolyte (SSE) is non-flammable and non-corrosive.[1–3] However, many of the recently well-studied SSEs are sulfide-based; while sulfide SSEs have an advantage over oxides in terms of ionic conductivity and ease of processability,[4–6] one main drawback is higher chemical reactivity and lower electrochemical stability, especially when used in conjunction with oxide cathode materials, as sulfides will inherently electrochemically oxidize once subjected to higher voltages during charging.[7,8]

One common strategy to mitigate unwanted reactions between the SSE and the oxide cathode is the implementation of a chemically inert, Li-ion conducting, and electronically-insulating coating on the cathode particles. Such a coating needs to have a much lower reactivity with the SSE (compared to the cathode) and must also be thin enough (~5 nm) to not drastically raise the overall impedance of the ASSB. For this purpose, cathode coatings such as $LiNbO_3$ (LNO), $LiAlO_2$, $LiTaO_3$, $Li_4Ti_5O_{12}$ (LTO), lithium borate (LBO), and others have been explored.[7,9–14] However, it is important to note that many of these cathode coatings are prepared via a solvent-based solution process. In this work, a new dry coating process for LBO was investigated on the cathode $LiNi_{0.8}Co_{0.1}Mn_{0.1}O_2$ (NCM811) The electrochemical performance of ASSBs, prepared using Li_6PS_5Cl (LPSCl) as the electrolyte and LiIn alloy as the anode, showed that the LBO coating improved the first cycle discharge capacity from 40 mAh/g to 126 mAh/g when compared to a similar cell with bare NCM811. Other characterization methods, such as scanning transmission electron microscopy (STEM) with electron energy loss spectroscopy (EELS), revealed a ~1–2 nm-thick conformal LBO coating and X-ray diffraction (XRD) demonstrated that chemical reactions between LPSCl and NCM811 were mitigated by the coating. This dry process opens a new avenue to fabricate protective cathode coatings to enable longer-lasting ASSBs.

Methods

Materials preparation.—As sulfide-based materials are sensitive to air and moisture (decomposing to form toxic gases such as H_2S), all synthesis and characterization steps were done within an argon-filled glovebox (MBraun MB 200B, $H_2O < 0.5$ ppm, $O_2 < 5.0$ ppm) unless otherwise stated.

Commercial LPSCl was obtained from NEI Corporation and used as received. Commercial, bare $LiNi_{0.8}Co_{0.1}Mn_{0.1}O_2$ (NCM811) was obtained from LG Chem. The dry coating process was conducted as follows: Boric acid (>99.5%, Sigma Aldrich) was mixed with the uncoated NCM811 cathode in an agate mortar and pestle for 5 min according to the predetermined final boron parts per million (ppm), hereby designated as: LBO B1 (875 ppm), LBO B2 (1800 ppm), and LBO B3 (3500 ppm). The mixture was subsequently heated at 300 °C for 5 h under ambient conditions to produce the LBO-coated NCM811.

To prepare the solution-processed $LiNbO_3$ (LNO) coating, stoichiometric amounts of lithium ethoxide (>95%, Sigma Aldrich) and niobium ethoxide (>99.95%, Sigma Aldrich) were added to NCM811 before dispersing in anhydrous ethanol. The solution was then stirred for 1 h and dried under vacuum, before heating at 450 °C for 1 h under ambient conditions to produce the 2 wt% LNO-coated NCM811 powder.

To prepare the composite cathodes, LPSCl was mixed with the LBO/LNO-coated NCM811 in an agate mortar and pestle (using either a 60:40 weight ratio of LPSCl:cathode without carbon, or a 66:33:1 weight ratio of LPSCl:cathode:carbon) for 5 min. To prepare the $Li_{0.5}In$ anode, stoichiometric amounts of stabilized lithium metal powder (FMC Lithium) and indium powder (>99.99%, Sigma Aldrich) were mixed in a glass vial using a vortex mixer for about 5 min.

Cell fabrication and electrochemical characterization.—To prepare the cells, LPSCl powder was pressed at 370 MPa in a 10 mm polyether ether ketone (PEEK) die using two titanium

---

plungers. Subsequently, 10 mg of the as-prepared cathode composite was added on one side of the LPSCl pellet and pressed at 370 MPa, followed by the application of 40 mg of LiIn on the other side of the electrolyte pellet and pressing at 120 MPa. The cell configuration was secured into a cell holder and connected to a Landhe CT2001 Battery cycler and analyzed with the Land v7.3 software. All cells were cycled at room temperature, inside the Ar glovebox, at 2.5–4.3 V vs Li/Li$^+$. For the rate studies, the first charge was done at 0.1 C, while the subsequent charging steps were done at 0.5 C. All the specific capacities mentioned in this work were calculated based on the electrode active material amount. Electrochemical impedance spectroscopy (EIS) was performed with a Solartron 1260 impedance analyzer for assembled half cells. An applied AC potential of 30 mV over a frequency range from 1 MHz to 0.1 Hz was used for the EIS measurement.

Characterization.—STEM-EELS was performed on a JEOL JEM-ARM300CF at 300 kV, equipped with double correctors. EELS spectra were acquired from a square area of $\sim$2 $\times$ 2 nm near the surface layer with an acquisition time of 0.01 s. To minimize possible electron beam irradiation effects, EELS spectra presented in this work were acquired from areas without pre-beam irradiation.

XRD was carried out by loading the powder sample into a 0.5 mm Boron-rich glass capillary tube (Charles Supper). The sample was flame-sealed to ensure no ambient air contamination. The samples were measured on a Bruker Kappa goniometer equipped with a Bruker Vantec 500 detector. The sample was placed in the Bragg−Brentano $\theta-\theta$ configuration and the measurement was carried out using Mo Kα radiation.

Results and Discussion

The schematic of the dry coating process is shown in Fig. 1. As detailed in the experimental part, the boron concentrations used in this study were 875 ppm (LBO B1), 1800 ppm (LBO B2) , and 3500 ppm (LBO B3). To show that the surface impurities were removed by the dry coating process via reaction with boric acid, STEM imaging and EELS were performed on both the bare and LBO-coated NCM811 and the data are shown in Fig. 2.

From the STEM images and STEM-EELS mapping of the bare NCM811 (Figs. 2d and 2f), there is a layer of carbon on the surface of the NCM811 particles that comes from surface species such as Li$_2$CO$_3$. The LBO-coated NCM EELS spectrum (Fig. 2g) does not exhibit a signal from C, but only signal from B. This is an indication that Li$_2$CO$_3$ is consumed during the coating process to ultimately form the LBO coating on the cathode material. Similar results were obtained with the LBO B3 coating and the results are shown in Fig. S1 (available online at stacks.iop.org/JES/167/130516/mmedia) of the Supplementary Information. STEM images and intensity plots along the surface of the coated NCM particle (Fig. S2, for both LBO B2 and LBO B3) show the presence of cation mixing, i.e. TM

diffusing beyond the LBO coating. This cation mixing layer is 4–5 nm in thickness for LBO B2 (Fig. 2c) but 10–12 nm for LBO B3; such an increased thickness could be potentially detrimental to cell performance as the resistance would increase. For this reason, further increases in the boron content were not considered.

As there is a wide variety of lithium borate compounds, EELS spectra were obtained to deduce which specific borate species was synthesized during the coating process (Fig. 3). LBO B2 most closely matches with the spectra from Li$_2$B$_4$O$_7$ and LiBO$_2$, while for LBO B3, a peak shift is observed (due to the increasing B content during the coating process). Nevertheless, since boron is a light element and many LBO compounds yield similar spectra, it is challenging to narrow down the exact species present.

To test its electrochemical performance, LBO-coated NCM811 was used in an ASSB configuration that contains Li$_{0.5}$In as the anode and LPSCl as the SSE. Figure 4 shows the first cycle charge-discharge voltage profile, rate capability, capacity retention, and EIS of the full cells. From the data, the LBO-coated NCM811 outperformed bare NCM811 in all instances, and LBO B2 was shown to have the highest capacity among the three concentrations tested, regardless of the C rate (Figs. 4b and S3). The lower capacity of LBO B1 can be attributed to a coating that is too thin, increasing the chances of incomplete coverage, and thus not all unwanted reactions are mitigated. As for LBO B3, the lower capacity compared to LBO B2 can be attributed to the significantly thicker coating layer, which would increase charge transfer resistance in the cell. EIS of the bare and LBO B2-coated cells are shown in Fig. 4d; significant impedance growth after 20 cycles is observed for the bare NCM811 cell, indicative of unwanted chemical reactions that result in resistive CEI products unfavorable for cell performance. There is still impedance growth in the LBO B2 cell (due to unavoidable LPSCl oxidation)[15] but it is comparatively mitigated. To verify that the performance degradation of the bare NCM811 and LPSCl is from a chemical reaction, air-sensitive capillary XRD was conducted and the data are shown in Fig. S4. It is clear that LPSCl has degraded when mixed with the bare cathode but remained intact when mixed with LBO B2. Thus, unwanted chemical reactions are prevented by the coating.

It is important to note that by using more active material and adding conductive additive (66:33:1 NCM:LPSCl:C weight ratio), the initial discharge capacity further increased from 124 to 160 mAh g^{-1} (Fig. S5). These initial results are promising and suggest that continued optimization of the cell setup would be even more beneficial for cycling performance.

Furthermore, a comparison between the commonly used, solution-processed LNO coating and the dry-coated LBO B2 NCM811 was conducted and shown in Fig. 5, with longer-term cycling in Fig. S6, which shows the superior cycling performance of LBO B2 compared with LNO. The dry-processed LBO thus shows great promise as a coating material for long-lasting Li ASSBs.
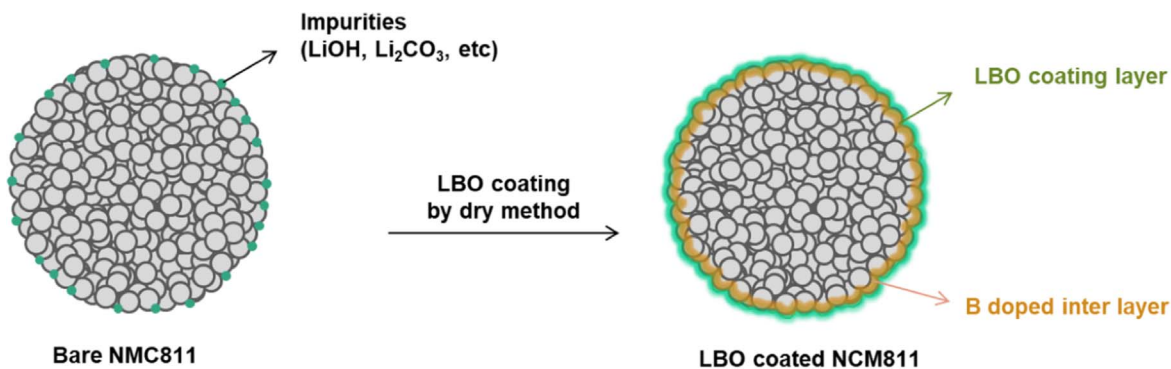
Figure 1. Schematic of the LBO coating process on NCM811 cathode particles through the simple dry coating method. Li-containing surface impurities are consumed during the coating process.
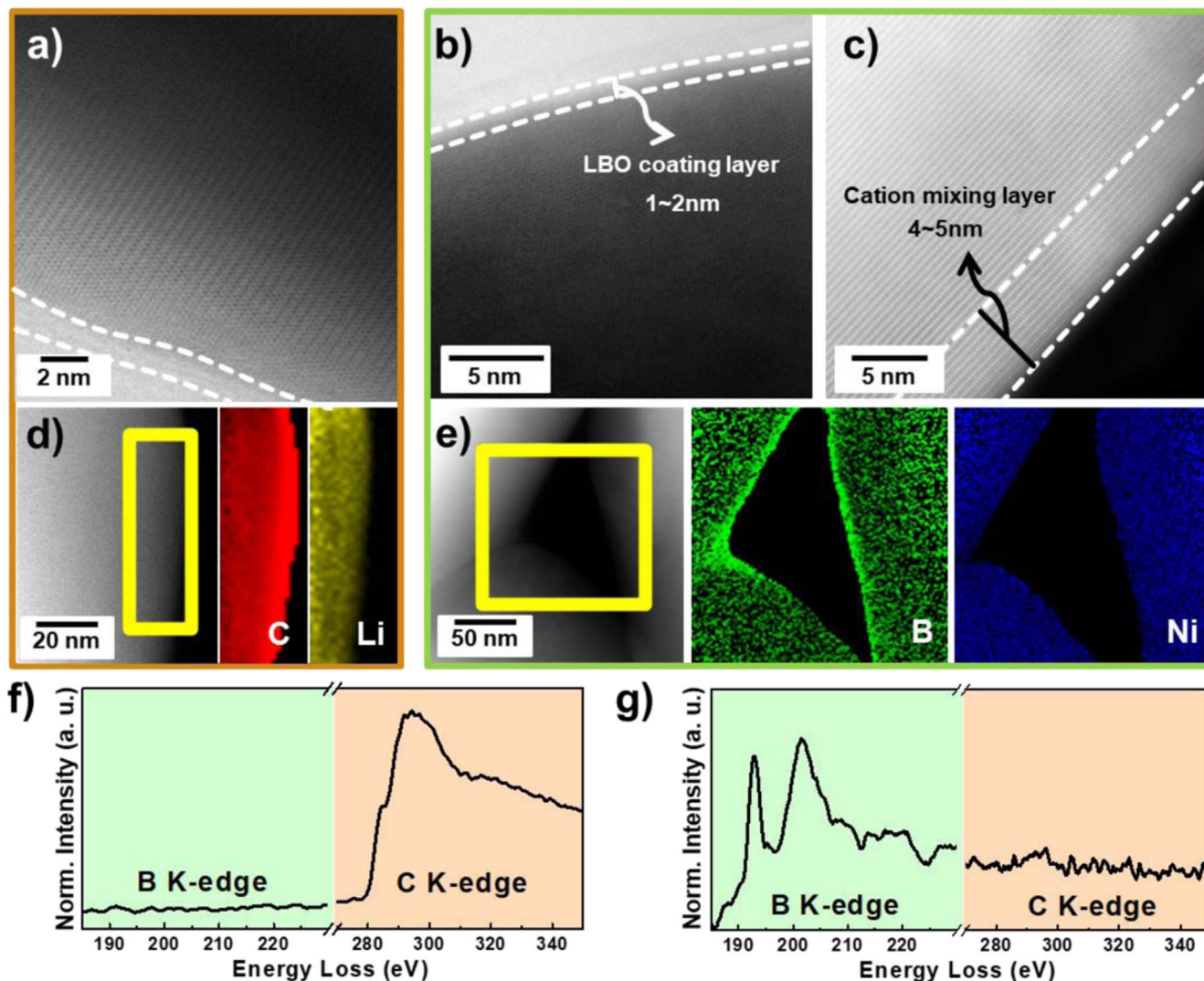
Figure 2. HAADF-STEM images of (a) Bare NCM811, (b) LBO B2-coated NCM, and (c) Boron-doped interlayer at the LBO B2-NCM surface. STEM-EELS elemental mapping of: (d) bare NCM at C K-edges and Li K-edges, (e) Intersection of three cathode particles of LBO B2-NCM for B K-edges and Ni L-edges. EELS spectra at the surface regions of: (f) bare NCM and (g) LBO B2-NCM.
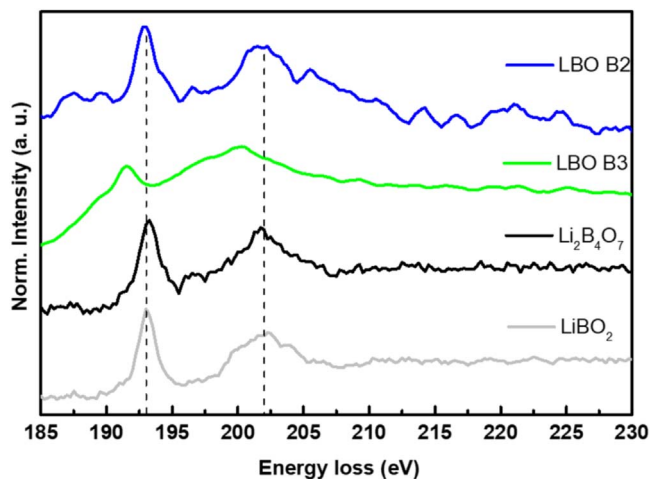
Figure 3. EELS spectra for LBO B2-coated NCM, LBO B3-coated NCM, $LiBO_2$, and $Li_2B_4O_7$ (latter two displayed for reference).

Conclusions

In sulfide-based all-solid-state batteries (ASSBs) that use an oxide cathode, it has been demonstrated that thin, conformal, and chemically inert oxide-based cathode coatings are beneficial for cycling performance as they mitigate unwanted chemical reactions between the SSE and the oxide cathode. Many coatings have been previously explored and applied to the cathode, usually via a solvent-based solution process. In this work, a dry-processed, lithium borate-based coating on NCM811 was shown to have the same desirable properties and even showed a higher first cycle capacity compared to the $LiNbO_3$-based solution-processed coatings. The LBO coating was synthesized by the solid-state reaction of boric acid with Li-containing impurities (such as Li_2CO_3) on the surface of NCM811, without the need for any washing or subsequent solvent removal. These results demonstrate the promise of both the facile dry-coating process and the LBO coating itself toward longer-lasting and better-performing ASSBs.
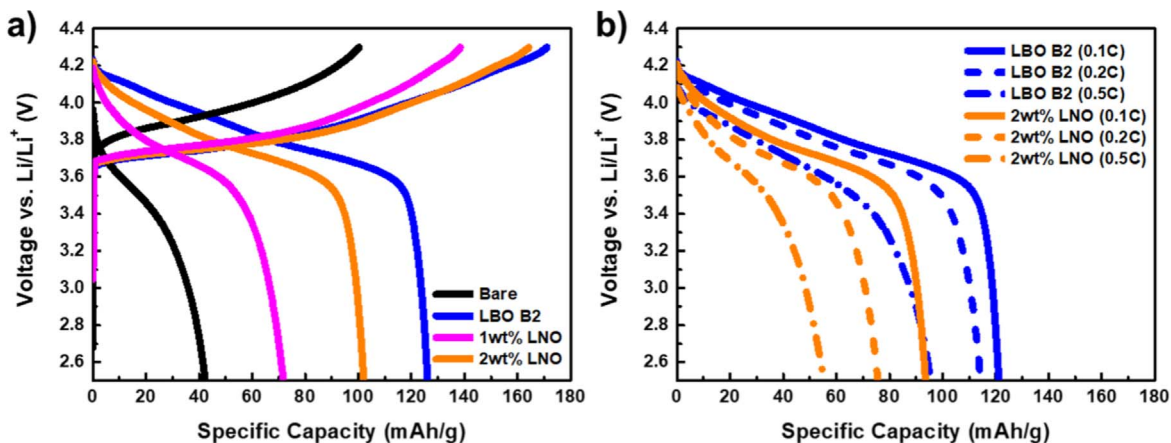
Acknowledgments
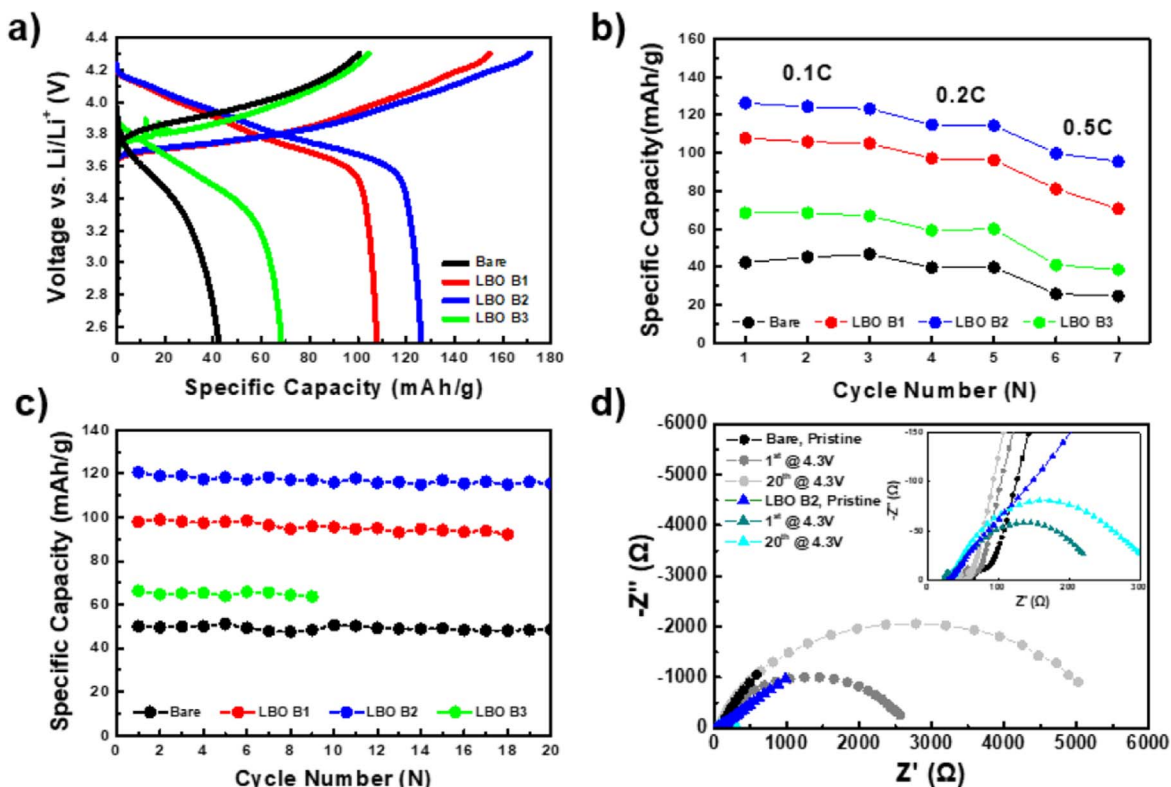
Figure 4. (a) Charge-discharge voltage profiles, (b) Rate capability, and (c) Cycle performance at 0.1 C of bare and LBO-coated NCM811 (with different boron concentrations) at 0.1 C. (d) Nyquist plots of bare and LBO B2-coated NCM811 before and after the 1st and 20th cycles. The cathode composites were prepared with a 60:40 weight ratio of NCM:SSE.

Figure 5. Comparison between bare, LBO B2 and LNO coating at 1 wt% and 2 wt%: (a) Charge-discharge voltage profiles. (b) Discharge voltage profile at various C rates.

assistance on the capillary XRD. The data is available from the corresponding author upon reasonable request.

ORCID

Ying Shirley Meng ⬤ https://orcid.org/0000-0001-8936-8845

References

1. Y. Guo, H. Li, and T. Zhai, "Reviving lithium-metal anodes for next-generation high-energy batteries." *Adv. Mater.*, **29**, 1700007 (2017).
2. J.-M. Doux, H. Nguyen, D. H. S. Tan, A. Banerjee, X. Wang, E. A. Wu, C. Jo, H. Yang, and Y. S. Meng, "Stack pressure considerations for room-temperature all-solid-state lithium metal batteries." *Adv. Energy Mater.*, **10**, 1903253 (2020).
3. L. Fan, S. Wei, S. Li, Q. Li, and Y. Lu, "Recent progress of the solid-state electrolytes for high-energy metal-based batteries." *Adv. Energy Mater.*, **8**, 1702657 (2018).
4. Y. J. Nam, S.-J. Cho, D. Y. Oh, J.-M. Lim, S. Y. Kim, J. H. Song, Y.-G. Lee, S.-Y. Lee, and Y. S. Jung, "Bendable and thin sulfide solid electrolyte film: a new electrolyte opportunity for free-standing and stackable high-energy all-solid-state lithium-ion batteries." *Nano Lett.*, **15**, 3317 (2015).
5. D. H. S. Tan et al., "Enabling thin and flexible solid-state composite electrolytes by the scalable solution process." *ACS Appl. Energy Mater.*, **2**, 6542 (2019).
6. H. Nguyen, A. Banerjee, X. Wang, D. Tan, E. A. Wu, J.-M. Doux, R. Stephens, G. Verbist, and Y. S. Meng, "Single-step synthesis of highly conductive Na$_3$PS$_4$ solid electrolyte for sodium all solid-state batteries." *J. Power Sources*, **435**, 126623 (2019).
7. W. D. Richards, L. J. Miara, Y. Wang, J. C. Kim, and G. Ceder, "Interface stability in solid-state batteries." *Chem. Mater.*, **28**, 266 (2016).
8. J. Lau, R. H. DeBlock, D. M. Butts, D. S. Ashby, C. S. Choi, and B. S. Dunn, "Sulfide solid electrolytes for lithium battery applications." *Adv. Energy Mater.*, **8**, 1800933 (2018).

9. K. Takada, N. Ohta, L. Zhang, K. Fukuda, I. Sakaguchi, R. Ma, M. Osada, and T. Sasaki, "Interfacial modification for high-power solid-state lithium batteries.." *Solid State Ion.*, **179**, 1333 (2008).

10. N. Ohta, K. Takada, I. Sakaguchi, L. Zhang, R. Ma, K. Fukuda, M. Osada, and T. Sasaki, "LiNbO$_3$-coated LiCoO$_2$ as cathode material for all solid-state lithium secondary batteries." *Electrochem. Commun.*, **9**, 1486 (2007).

11. B. Huang, Z. Zhao, Y. Sun, M. Wang, L. Chen, and Y. Gu, "Lithium-ion conductor LiAlO$_2$ coated LiNi$_{0.8}$Mn$_{0.1}$Co$_{0.1}$O$_2$ as cathode material for lithium-ion batteries.." *Solid State Ion.*, **338**, 31 (2019).

12. Y.-R. Zhu, T.-F. Yi, R.-S. Zhu, and A.-N. Zhou, "Increased cycling stability of Li$_4$Ti$_5$O$_{12}$-coated LiMn$_{1.5}$Ni$_{0.5}$O$_4$ as cathode material for lithium-ion batteries." *Ceram. Int.*, **39**, 3087 (2013).

13. X. Li, J. Liu, M. N. Banis, A. Lushington, R. Li, M. Cai, and X. Sun, "Atomic layer deposition of solid-state electrolyte coated cathode materials with superior high-voltage cycling behavior for lithium ion battery application." *Energy Env. Sci*, **7**, 768 (2014).

14. H.-W. Chan, J.-G. Duh, and S.-R. Sheen, "Electrochemical performance of LBO-coated spinel lithium manganese oxide as cathode material for li-ion battery." *Surf. Coat. Technol.*, **188–189**, 116 (2004).

15. D. H. S. Tan, E. A. Wu, H. Nguyen, Z. Chen, M. A. T. Marple, J.-M. Doux, X. Wang, H. Yang, A. Banerjee, and Y. S. Meng, "Elucidating reversible electrochemical redox of Li$_6$PS$_5$Cl solid electrolyte." *ACS Energy Lett.*, **4**, 2418 (2019).